DESIGN OF ACTIVE-FEEDBACK LOW NOISE AMPLIFIER WITH IMPROVED LINEARITY

Nuhu Umar Elisha[1], Mutari Hajara Ali[2]
[1]PG Electronics Student, [2]Professor
Department of Physics
Bayero University Kano, Nigeria.

***Abstract*:** The application of active feedback using source follower provides wide bandwidth. However, the source follower introduces non-linearity within the passband. This study proposes a way to mitigate this problem through the use of a resonant tank connected along the feedback path, which exploit the blocking capacity of the capacitor to linearize the source follower. Also, we adopted the inductive peaking technique for bandwidth enhancement, noise performance improvement and circuit stability. With the combination of these techniques, an improved linearity for the active feedback low noise amplifier for wideband receivers was achieved while improving the noise performance. Simulated result of the low noise amplifier showed a power gain of 13.13dB and a 3dB bandwidth of 16.88MHz. It achieved an input return loss < -10dB, reverse isolation better than -23.4dB, output return loss < -14dB. Output total RMS noise achieved is 9.1μV while dissipating and average of 67.512mW from a 9V supply. The simulated result for both input and output return losses are < -10dB, this implies good impedance matching at both input and output of the LNA. This work shows it is possible to linearize an active feedback LNA by adding a resonant tank along the feedback path.
Keywords: Active-Feedback, Low noise amplifier, resonant tank linearization, linear, wideband.

1.0 INTRODUCTION

The first block in the receiver architecture is the low noise amplifier with high gain and good input impedance matching. In the last few decades, several wireless standards have been implemented while the frequency spectrum is becoming less and less due to congestion (Huang, Yang, Chen, Khan, & Lin, 2018), this has drawn much attention to research on software defined radio (SDR) in the past few decades. The first software defined radio was proposed by Mitola (Mitola, 1995), this was not achieved due to the difficult requirement on analog to digital converters (Arshad, Zafar, Ramzan, & Wahab, 2013). The wideband has many applications such as UHF TV; cellular phones; radar; microwave links; personal communications services (Vaithianathan, Raja & Srivivasan, 2012). Meanwhile, signals processed over the wideband are not immune to signal attenuation and noise. Hence, the receiver front-end must be an amplifier with high gain and low noise characteristics, precisely the low noise amplifier (LNA). Wideband receivers normally require sufficient linearity over the desired band to protect out-of-band interferes from generating intermodulation product and other noises.

The design of wideband LNA is a challenging process in several aspects, this includes; having a low noise figure (NF), supplying proper input and output matching, power consumption and maintaining high linearity (Arshad et al., 2013). Also, LNA design is challenging due to the short-channel effects in metal oxide semiconductor (MOS) devices, reducing supply voltages and Low-Q of the on-chip passives that degrade the RF circuit parameters (Razavi, 2015). Several techniques have been reported to meet this stringent requirement for LNA design. Common gate (CG) LNA has been investigated widely, because it has inherent good wideband matching, linearity, and stability. However, the noise figure (NF) of a CG-LNA is relatively high due to the input matching condition gm=1/*RS*, the gain is also low due to limited g_m (Ma, Wang, Xu, & Amin, 2016). Noise-canceling LNA is a good option for the wideband impedance matching with a low NF. This LNA cancels its thermal noise and nonlinear harmonic distortion induced by the first stage transistors using a negative feedback (Bruccoleri, Klumperink & Nauta, 2004). However, it is hard to eliminate the distortion generated from an auxiliary amplifier which is the main nonlinear element (Chung & Lee, 2015). Distributed amplification was used for bandwidth extension was adopted (Lin, Chang, & Lu, 2011), however such distributed amplification consumes much energy leading to high power dissipation (Sahafi, Sobhi, and Koozehkanani, 2016)

The active-feedback topology can alleviate the common tie between gain and noise figure (NF) with good input matching. However, it has been proved (Borremans, Wambacq, Soens, Rolain, & Kuijk, 2008) that the feedback is nonlinear and causes a large fraction of distortion because of the feedback transistor's nonlinearity, this result in poor linearity. Thus, making the active-feedback LNA not suitable for wideband receivers.

Within the last decade, several methods have been presented to meet the linearity requirement of wideband LNAs. Some of the linearization techniques reported in open literature includes; derivative superposition (DS) (Guo, Chen, Li, Jin, & Yang, 2017). This technique improved the linearity (IIP3 of 8.3–10 dBm) with severe bandwidth reduction. Complementary derivative superposition was proposed (CDS) (Guo & Chen, 2017), while this improved the bandwidth, there was deterioration in power consumption. Noise/distortion cancellation were used by (Ebrahimi, Bastan, Ebrahimi, & Shamsi, 2014; Hayati, Cheraghaliei, & Zarghami, 2017; Seyedi, Dehdasht-heydari, & Roshani, 2019), this technique only provided slight improvement in IIP3 while dissipating unacceptable power. Pre-distortion (Jafarnejad, Jannesari, & Sobhi, 2017b) and post-distortion (Amirabadi, Zokaei, Bagheri, & Alirezazadeh, 2015; Guo, Wen, & An, 2014). A highly linear complementary source follower (CSF) feedback CMOS wideband LNA was proposed (Im, 2013) and implemented as a part of a highly linear receiver front-end. This topology achieved high linearity with high power dissipation and limited passband. Huang, Yang, Chen, Imran and Lin., (2018) proposed a complementary source follower to mitigate the problem of active feedback nonlinearity and power consumption. The work presented a good result while dissipating moderate power. These methods have been used as tradeoff between gain, linearity and power consumption.

In this study, a linear low noise amplifier is designed using the active negative feedback technique for bandwidth enhancement, gain stabilization and input matching. A resonant tank is used to improve the linearity of the common source follower. Furthermore, an inductive peaking technique was used for bandwidth enhancement, noise improvement and circuit stability.

2.0 LNA DESIGN CHALLENGES

Design of a wideband low noise amplifier is a very challenging process in aspects, this includes; having a low noise figure (NF), supplying proper input and output matching, power consumption and maintaining high linearity (Arshad *et al*., 2013). It is also essential that the design attain reasonable gain and stability without oscillation over entire useful frequency range (Singh & Katare, 2017). Achieving a wideband can also be very challenging. Over the years, several techniques have been proposed for bandwidth enhancement such as series peaking, shunt peaking, shunt-series, T-coil and fT-doublers using Darlington pairs (Vaithianathan *et al*, 2012). LNA design should meet several challenges like good transistor selection, high gain, suitable DC biasing network and good stability. The design trade-off is summarized in figure below.

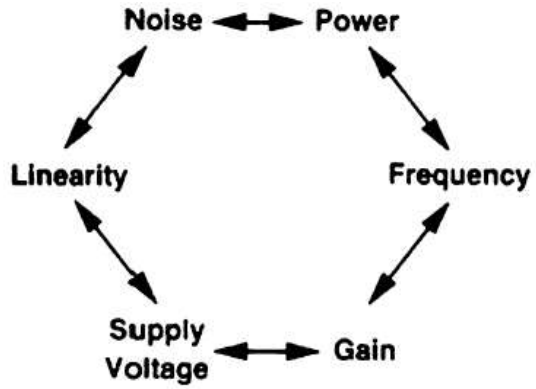

LNA design matrix

Design specifications for a state-of- the-art wideband LNAs include:

i. Minimum signal reflection by achieving good (50 Ω) input matching (S11 ≤ −10dB) for all frequencies (Sapone & Palmisano, 2011).
ii. NF ≤ 3.5dB over the entire bandwidth (Roovers *et al*., 2005)
iii. Higher linearity (IIP3 ≥ 0dBm) (Brandolini, Rossi, Manstretta & Svelto., 2005)
iv. Minimal signal reflection by achieving good output matching (S22 ≤ -10dB) for all frequencies (Yusof, Fauzi, Mohamed, Faiz, & Omar, 2020)
v. Flat gain across the entire bandwidth (Bevilacqua & Niknejad, 2004)
vi. High IIP2 ≥ 40dBm in case of Zero IF architecture (Abidi, 2003).
vii. Unconditional stability over entire frequency range.

These requirements must be fulfilled without any compromise on silicon area and power consumption. In wideband LNAs, the need of a large bandwidth imposes significant challenges compared to narrow band or multiband LNA (Arshad et al., 2013).

3.0 CIRCUIT DESIGN

The proposed low noise amplifier schematic is shown in fig. 4. It is designed with a common source cascode structure (M1 and M2) to increase the output impedance and also reduce the miller effect impact on the input stage, with an active feedback (M3) in a common drain configuration. Bandwidth enhancement with inductive shunt-peaking is adopted by connecting an inductor in series with a resistive load. Figures 1and 2 shows the common source stage and the hybrid-pi model, analysis of the small-signal voltage gain of the common source is given thereafter.

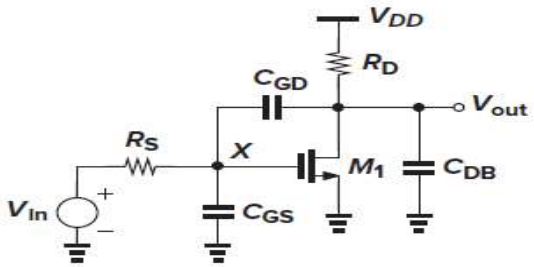

Fig. 1. Common source Amplifier.

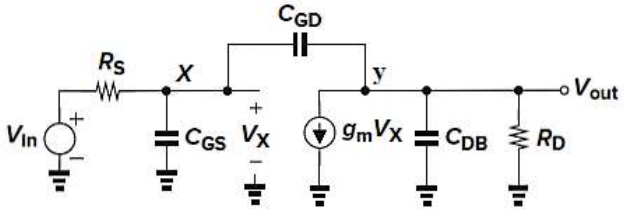

Fig. 2. Complete hybrid-pi model of the common source amplifier.

3.1 Circuit Analysis

Analysis of the circuit topology used in this design is given below

3.1.1 Gain of the Amplifier

From figure 2 above,

At node X, applying KVL

$$\frac{V_x - V_{in}}{R_s} + V_x s C_{gs} = (V_{out} - V_x) s C_{gd} \quad (1)$$

Rearranging equation (1)

$$\frac{V_x - V_{in}}{R_s} + V_x s C_{gs} + (V_{out} - V_x) s C_{gd} = 0 \quad (2)$$

At node Y, applying KVL,

$$(V_{out} - V_x) s C_{gd} + g_{mcs} V_x + \frac{V_{out}}{R_d} + V_{out} s C_{db} = 0 \quad (3)$$

Simplifying equation (3) for V_x,

$$g_{mcs} V_x - s V_x C_{gd} + s V_{out} C_{gd} + \frac{V_{out}}{R_d} + s V_{out} C_{db} = 0$$

$$V_x = \frac{-V_{out}\left(\frac{1}{R_d} + s C_{gd} + s C_{db}\right)}{g_{mcs} - s C_{gd}} \quad (4)$$

From equation (2),

$$\frac{V_x}{R_s} - \frac{V_{in}}{R_s} + s V_x C_{gs} + s V_x C_{gd} - s V_{out} C_{gd} = 0$$

$$V_x \left(\frac{1}{R_s} + s C_{gs} + s C_{gd}\right) - s V_{out} C_{gd} - \frac{V_{in}}{R_s} = 0 \quad (5)$$

Substitute equation (4) into (5) for V_x,

$$\frac{-V_{out}\left(\frac{1}{R_d} + s C_{gd} + s C_{db}\right)}{g_{mcs} - s C_{gd}} \left(\frac{1}{R_s} + s C_{gs} + s C_{gd}\right) - s V_{out} C_{gd} - \frac{V_{in}}{R_s} = 0$$

$$-V_{out} \frac{\left(\frac{1}{R_d} + s C_{gd} + s C_{db}\right)\left(\frac{1}{R_s} + s C_{gs} + s C_{gd}\right) - s V_{out} C_{gd}\left(g_{mcs} - s C_{gd}\right)}{g_{mcs} - s C_{gd}} = \frac{V_{in}}{R_s} \quad (6)$$

Simplifying equation (6)

$$-V_{out}\left(\frac{1}{R_d R_s} + \frac{s C_{gs}}{R_d} + \frac{s C_{gd}}{Rd} + \frac{s Cgd}{Rs} + s^2 C_{gs} C_{gd} + s^2 {C_{gd}}^2 + \frac{s C_{db}}{Rs} + s^2 C_{gs} {C_{db}}^2 + s^2 C_{db} C_{gd}\right) - \left(g_{mcs} - s C_{gd}\right) s V_{out} C_{gd}$$
$$= V_{in} \frac{\left(g_{mcs} - s C_{gd}\right)}{R_s} \quad (7)$$

Solving equation (7) for the voltage gain of the amplifier

$$A_v = \frac{V_{out}}{V_{in}} \tag{8}$$

$$A_v = \frac{V_{out}}{V_{in}} = -\frac{(g_{mcs} - sC_{gd})R_d}{(1 + sR_sC_{gs} + s(C_{gd} + R_d g_{mcs} C_{gd})R_s + s(C_{gd} + C_{db})R_d + s^2 R_d R_s \alpha)} \tag{9}$$

Where $\alpha = (C_{gs}C_{gd} + C_{gs}C_{db} + C_{gd}C_{db})$,

$$A_v = \frac{(sC_{gd} - g_{mcs})R_d}{(1 + sR_sC_{gs} + s(C_{gd} + R_d g_{mcs} C_{gd})R_s + s(C_{gd} + C_{db})R_d + s^2 R_d R_s \alpha)} \tag{10}$$

Neglecting the transistor capacitances, the voltage gain is given by the equation below

$$A_v = -g_{mcs}R_d \tag{11}$$

When the amplifier is designed with a resistive load R_l, then equations (10) and (11) can be modified as below

$$A_v = \frac{(sC_{gd} - g_{mcs})R_l}{(1 + sR_sC_{gs} + s(C_{gd} + R_l g_{mcs} C_{gd})R_s + s(C_{gd} + C_{db})R_l + s^2 R_l R_s \alpha)} \tag{12}$$

$$A_v = -g_{mcs}R_l \tag{13}$$

where,

R_s and R_d are the source and drain (load) resistance respectively.

C_{gs}, C_{gd}, C_{db} are the gate to source, gate to drain and drain to body capacitances respectively.

g_{mcs} is the transconductance of the common source transistor.

The active feedback network is shown below

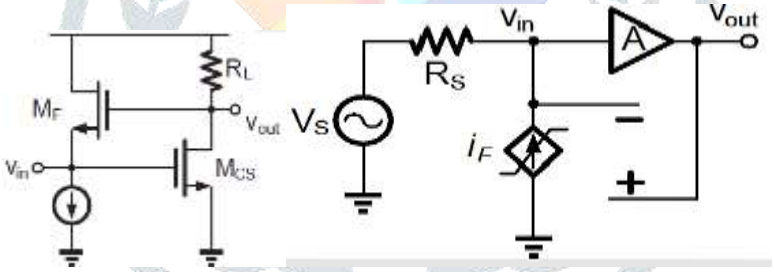

Fig. 3(a). Traditional active-feedback Fig. 3(b). AC equivalent circuit

3.1.2 Input Impedance matching

The input impedance of the amplifier is designed with active shunt feedback. It can be proven out from the equivalent circuit of figure 3(b) (reactive components excluded for simplicity) above that the input impedance is obtained as follows;

$$V_{out} = I_d R_l = -g_{mcs}V_{in}R_l = g_{mcs}R_l V_{in} \tag{14}$$

But $-g_{mcs}R_l = A_v$

From equation (8),

$$V_{out} = A_v V_{in} \tag{15}$$

Considering the feedback network,

$$I_{df} = g_{mf}(V_{out} - V_{in}) \tag{16}$$

$$I_{df} = g_{mf}(-g_{mcs}R_l V_{in} - V_{in})$$

$$I_{df} = -g_{mf}(g_{mcs}R_l + 1)V_{in} \quad (17)$$

But $I_{in} = -I_{df}$

$$I_{in} = -I_{df} = -g_{mf}(g_{mcs}R_l + 1)V_{in}$$

$$I_{in} = g_{mf}(g_{mcs}R_l + 1)V_{in}$$

$$Z_{in} = \frac{V_{in}}{I_{in}} = \frac{1}{g_{mf}(g_{mcs}R_l + 1)} = \frac{1}{g_{mf}(g_{mcs}R_l + 1)} \quad (18)$$

$$Z_{in} = \frac{1}{g_{mf}(1 + |A_v|)} \quad (19)$$

Equation (13) shows that the gain is determined by the common source stage of the amplifier while equation (19) shows that the input impedance is dominated by the feedback transistor. Hence, for good matching, the transconductance of the feedback transistor should be kept constant and $Rs = Z_{in}$. The complete proposed LNA circuit is shown in fig. 3 which is simulated in LTSpice XVII model. The capacitors C_1 through C_4 are all DC blocking capacitors, C_5 and R_7 formed the resonant tank used to improve the linearity of the active-feedback LNA.

3.1.3. Noise Analysis

The noise factor of the amplifier is essential as it determine the dominating factor in the noise of the amplifier. In this analysis we assume the cascode amplifier has no noise contribution at the out. Also, we assume the linear current source used is noiseless. The noise factor F of the LNA is given by the individual noise contributions of the M1, M3, R1, RS. A theorical expression for the noise figure of a single-ended version of our design is derived from (Razavi 2001), reactive component excluded.

$$F = \frac{\sum V^2 n}{V^2_{n,Rs}} \quad (20)$$

Hence, the noise factor is given by,

$$F = F_{Rs} + F_{mcs} + F_{mf} + F_{R1} \quad (21)$$

$$F = 1 + \frac{\gamma_{mcs}R_s}{g_{mcs}}\left[\frac{1}{Rs} - g_{mf}\right].^2 + \frac{\gamma_f g_{mf}R_s}{1} + \frac{Rs}{g_{mcs}A_v}[\frac{1}{Rs} + g_{mf}]^2 \quad (22)$$

For impedance matching, the source impedance must match the input impedance

$$Z_{in} = R_s = \frac{1}{g_{mf}(1 + g_{mcs}R_l)} = \frac{1}{g_{mf}(1 - A_v)} \quad (23)$$

Making g_{mf} the subject

$$g_{mf} = \frac{1}{R_s(1 - A_v)} \quad (24)$$

Imposing the matching criterion of equation (23) on equation (22) and substituting equation (24) into (22) for g_{mf},

$$F = 1 + \frac{\gamma_{mcs}R_s}{g_{mcs}}[\frac{1}{R_s} + \frac{1}{R_s(1 - A_v)}]^2 + \frac{\gamma_f R_s}{R_s(1 - A_v)} + \frac{R_s}{g_{mcs}A_v}[\frac{1}{R_s} + \frac{1}{R_s(1 - A_v)}]^2$$

$$F = 1 + \frac{\gamma_{mcs}}{g_{mcs}R_s}[\frac{2 - Av}{1 - Av}]^2 + \frac{\gamma_f}{(1 - A_v)} + \frac{1}{g_{mcs}A_v R_s}[\frac{2 - A_v}{1 - A_v}]^2 \quad (20)$$

where γ_{mcs}, γ_f, are the thermal noise coefficient of M_{cs}, and M_f respectively, it can be seen that a larger g_{mcs} will lead to a low noise factor. However, this will involve taking a larger overdrive voltage (V_{gs} - V_{th}) leading to higher power dissipation which is not desired.

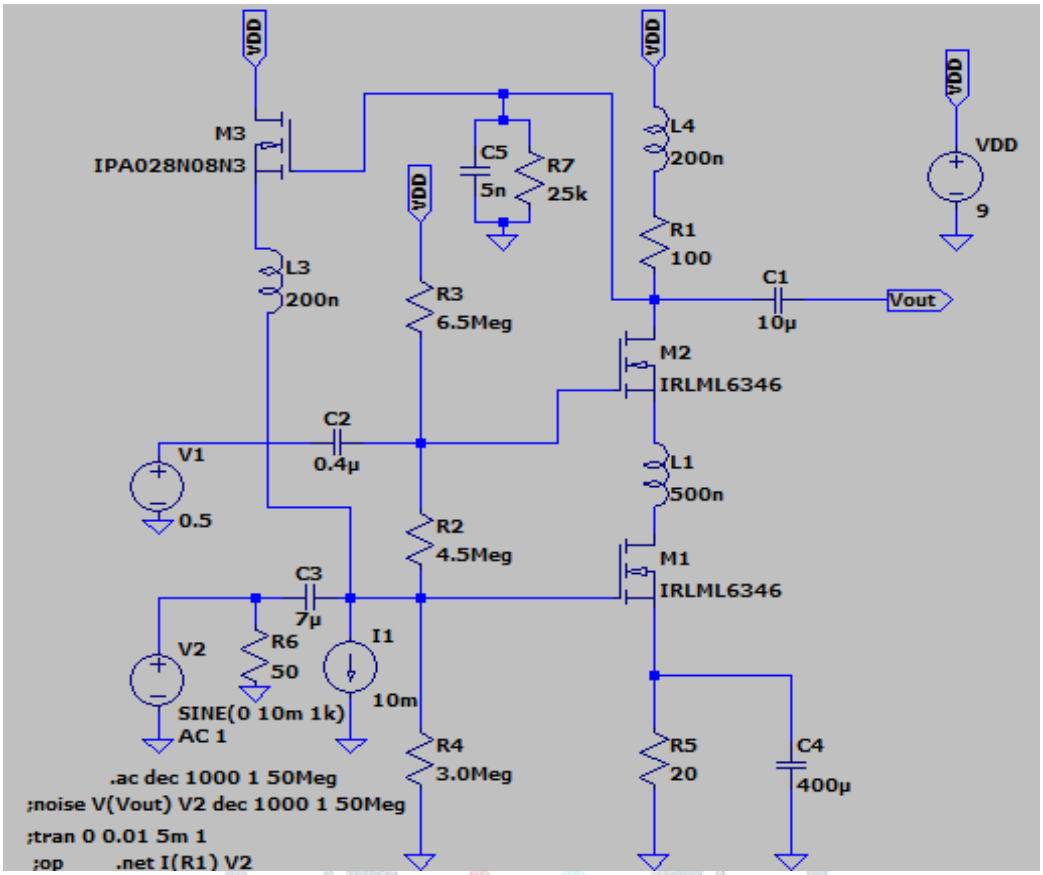

Fig. 4. complete schematic of the proposed LNA.

4.0 RESULT AND DISCUSSION

4.1 Simulation Result for a single stage Common source amplifier

The simulated result for a single stage common source amplifier is shown below.

Simulation using LTSpice Simulator and MATLAB

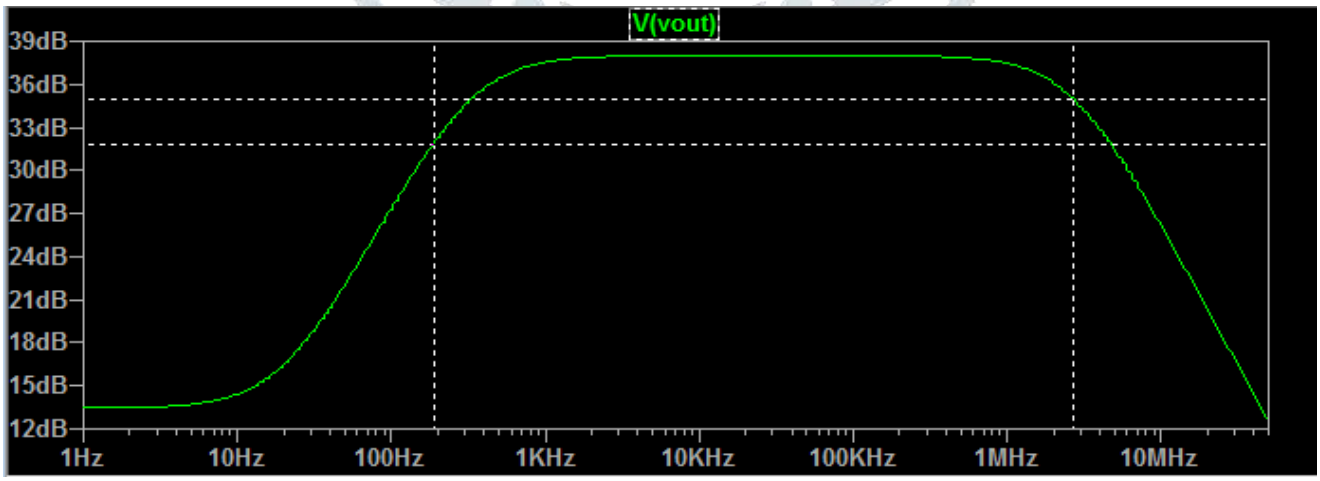

Fig. 5. Voltage transfer function of the single stage amplifier

We generated a MATLAB code of the transfer function for equation 12 and ran it to generate the bode plot for the voltage gain. The result obtained is shown below in figure 6.

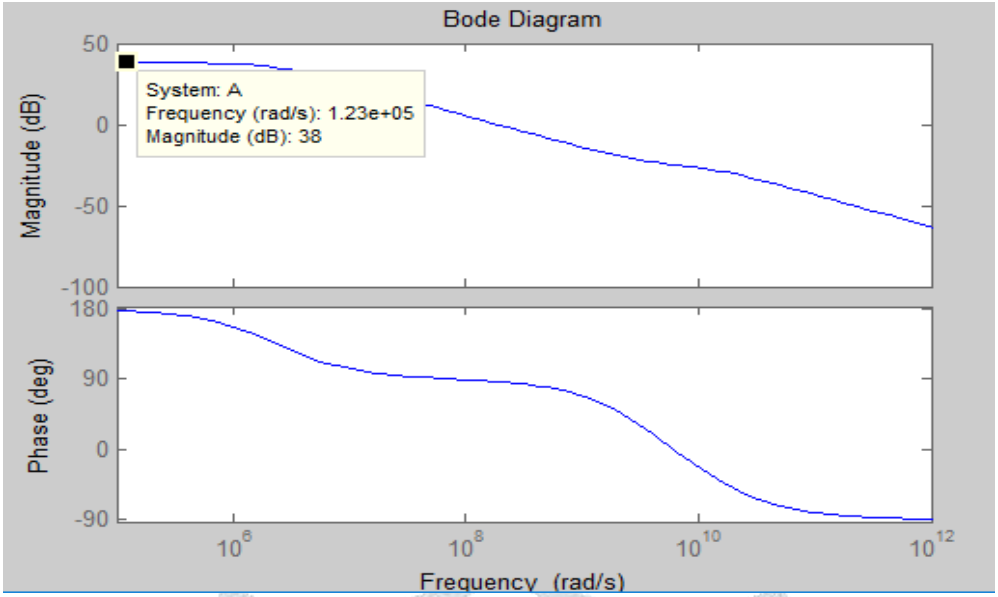

Fig. 6. MATLAB simulated result for the Common source amplifier.

From figures 5 and 6, the voltage gain for the LTSpice simulator and MATLAB code are 37.9965dB and 38dB respectively. This imply that both simulators are in close agreement and thus validate the design and performance of the LTSpice simulator. From the LTSPice simulator, the passband is 2.7288MHz with a power gain of 24.03dB.

4.2 Simulated result of the active-feedback LNA.

To extend the passband, active feedback topology with inductive peaking technique for bandwidth enhancement, noise improvement and circuit stability was adopted, the simulated result is given below.

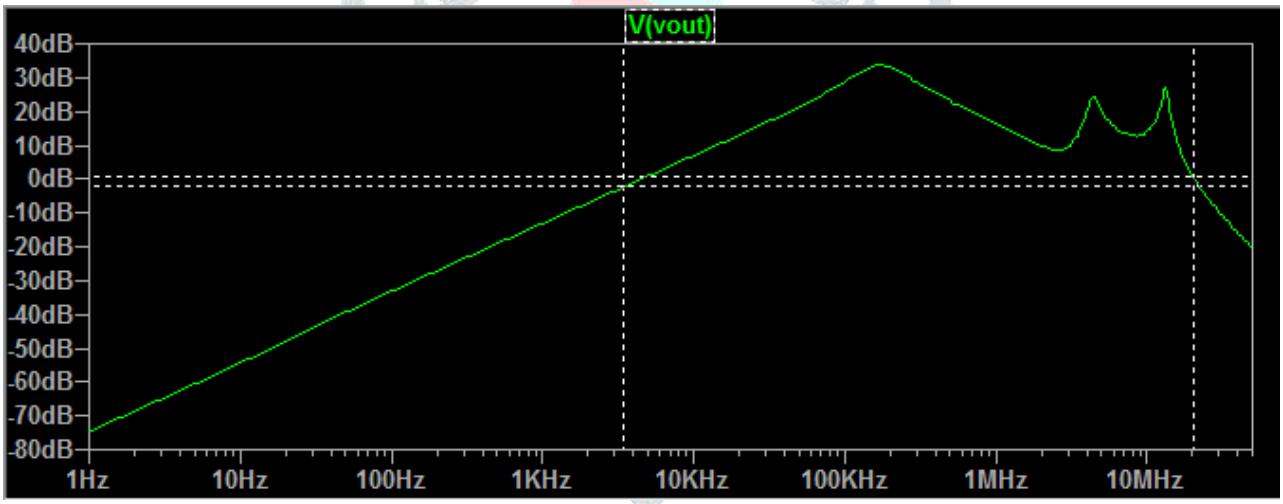

Fig. 7. Frequency response of active-feedback LNA

From figure 7 above, it is seen that with the application of active feedbck, the passband is 20.414MHz with a power gain of 16.86dB. Though, there is a drop in the power gain, bandwidth extention extension has fully compensated for the power loss. The downside of this topology is the nonlinear response of the gain as can be seen from the passband above and additional power dissipation. This nonlinearity is as a result of interaction between the gate-to-drain capacitor (Cgd) of the common source amplifier and the gate-to-source capacitor (Cgs) of the feedback transistor producing an equivalent capacitance sufficient to to cause oscillation within the passband of interest. To mitigate this problem of nonlineaity, we adopted the use of a resonant tank placed in the feedback path. This tank ground the noise before reaching the feedback device.

4.3 Simulated result of the active-feedback LNA with linearization.

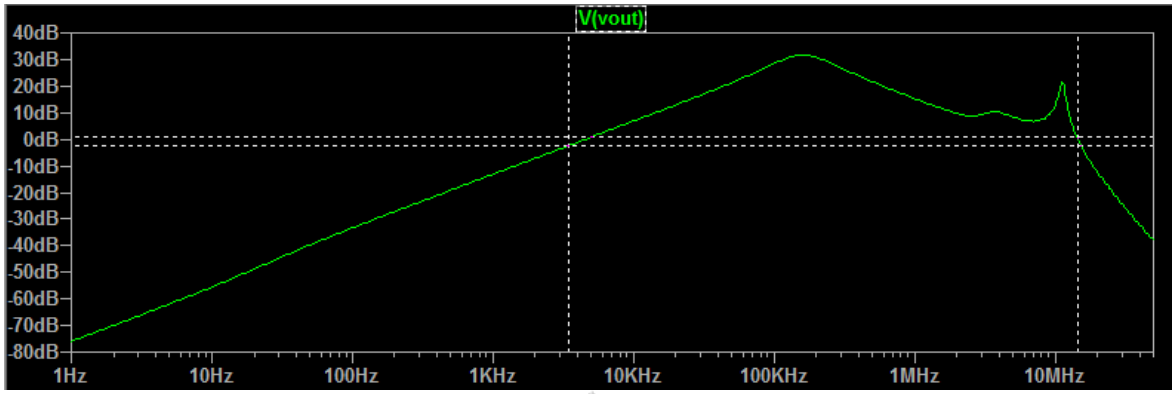

Fig. 8. Simulated result of Voltage gain for the active-feedback with linearization\

Figure 8 above shows that the application of the linearization technique yielded significant result. In this approach, the resonant tank grounds the noise thus, preventing it from reaching the feedback device and hence stopping further amplification of the noise leading to the nonlinearity seen in the passband of figure 7. The achieved bandwidth with this linearization technique is 16.8655MHz with a power gain of 13.13dB. Other parameters that defines the success of the design of an LNA are compared for the active-feedback LNA without and with linearization

4.4 Scattering Parameters

The S-Parameter describe the response of an n-port network to signal incidented to any or all of it ports. The first number in the subscript refers to the responding port while the second number is the incident port. Its simulation shows the electrical behaviour of an electrical circuit. Figures (9 and 10) shows the simualated result of the scattering parameters for the active-feedback LNAs without and with linearization technique. The input return losses (S_{11}) simulated result for the LNAs without and with linearization shows that both topology have good input matching since S_{11} < -10dB for both LNAs. Also, for the output return losses for the LNAs without and with linearization, the result indicate good output matching for the topology without linearization (S_{22} < -10dB), while for the active-feedback LNA shows that the output matching not so good as S_{22} > -10dB. The reverse isolation (S_{12}) simulated result shows a good reverse isolation for the LNAs. The LNAs without linearization and with linearization achieved S_{12} is better than -20dB and -28dB respectively within the passband. These shows that the output matching of the active-feedback LNA was traded for reverse isolation. The simulated power gain (S_{21}) result for both LNAs indicates that both achieved a good power gain with both S_{21} > 10dB.

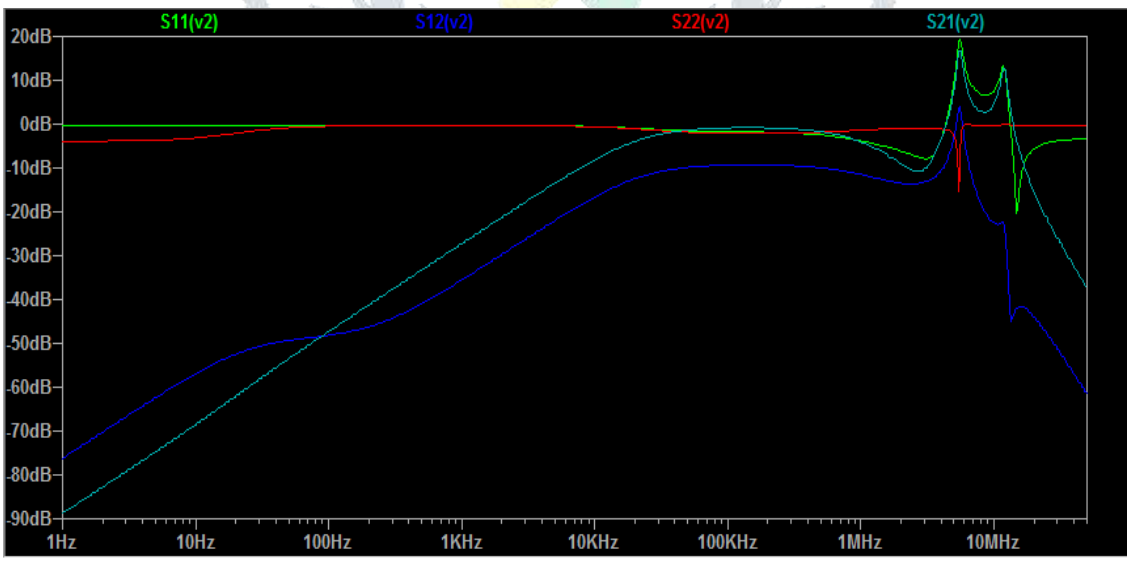

Fig. 9. Simulated result of the S-Parameter for Active-feedback LNA without linearization

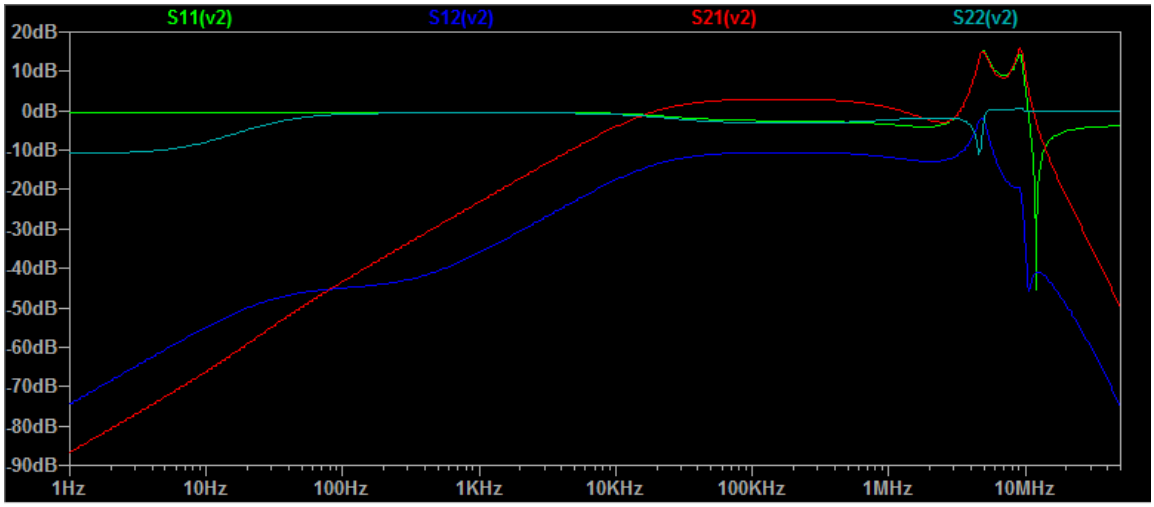

Fig. 10. Simulated result of the S-Parameter for Active-feedback LNA with linearization

4.5 Power dissipation

The power dissipation of an LNA is very critical to designers. It is essential that power dissipation of the transistors be minimized during design such that it does not reach it maximum power dissipation. Figures (11 and 12) shows the simulated result of the power dissipation for both LNAs without and with linearization technique. It can be seen that with this new design approach power dissipation is very much minimized. The additional power dissipation is 0.035mW. This a better improvement to other reported techniques.

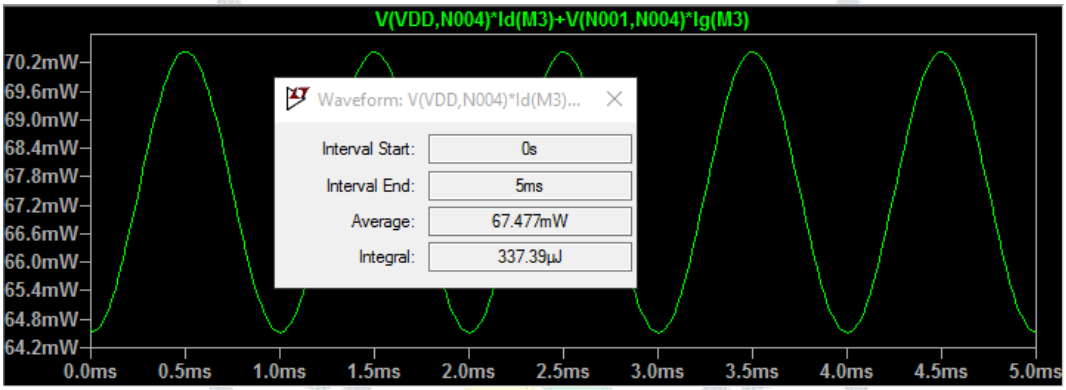

Fig. 11. Power dissipation of Active-Feedback LNA without Linearization

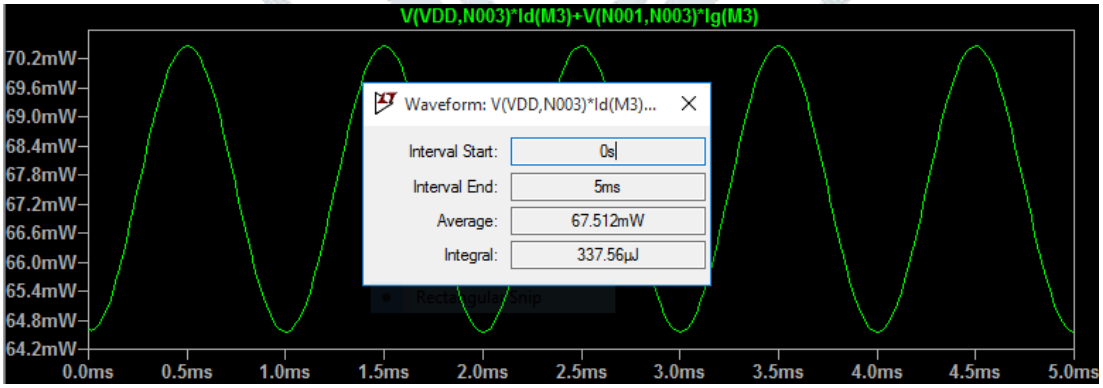

Fig. 12. Power dissipation of Active-Feedback LNA with Linearization

4.6 Noise

Since LNAs are designed to amplify weak signals without adding much noise to the signal to enable data retrieval, the noise performance of the LNA is very critical to the success of the design. Figures (13 and 14) shows the simulated result of the output noise for the LNAs without and with linearization technique. Comparing the result, it is clear that this technique does not only improve the nonlinearity within the passband but also reduces the noise generated. Thus, with this technique, there is improvement in the nonlinear response of the amplifier and the noise.

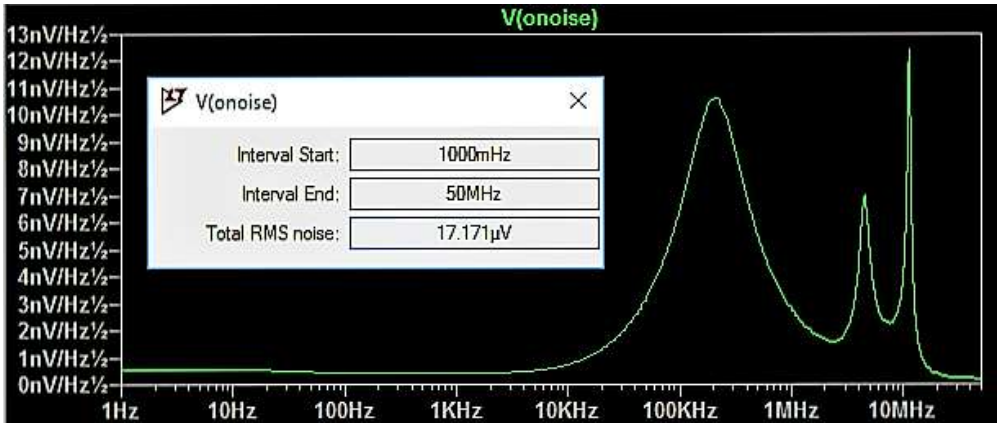

Fig. 13. Output noise of the Active-feedback LNA without linearization

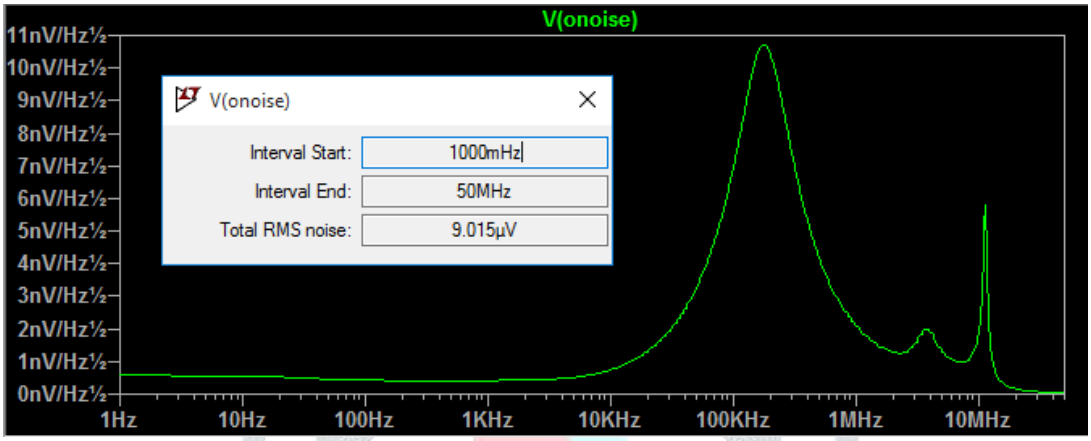

Fig. 14. Output noise of the Active-feedback LNA with linearization

5.0 Conclusion

In conclusion, we found that the addition of resonant tank along the feedback path mitigates the nonlinearity introduced by the source follower in the active feedback low noise amplifier. This result is because of the reduced circuit component and less noise. With this approach, there is reduction in cost, chip size, power consumption. At the end of this study, a linear active feedback low noise amplifier employing the resonant tank technique for linearization was achieved. This will provide better signal reception using the wideband. Also, this technique can be used in the design of wideband LNA to achieve bandwidth in GHz in submicron CMOS technologies.

REFEFENCES

[1]. Abidi, A A. (2003). General Relations Between IP2 , IP3 , and Offsets in Differential Circuits and the Effects of Feedback. *IEEE Trans. Microwave Theory Tech*, 51(5): 1610–1612.

[2]. Amirabadi, A., Zokaei, A., Bagheri, M., and Alirezazadeh, F. (2015). Highly Linear Wide-Band Differential LNA Using Active Feedback as Post Distortion. IEEE J Solid-State Circuits, 40(6) 654–657.

[3]. Arshad, S., Zafar, F., Ramzan, R., and Wahab, Q. (2013). Wideband and multiband CMOS LNAs : State-of-the-art and future prospects. *Microelectronics Journal*, 21(4): 1–13. https://doi.org/10.1016/j.mejo.2013.04.011

[4]. Behzad Razavi (2001). Design of Analog CMOS Integrated Circuits, *McGraw-Hill, 2001*, ISBN 0-07-118815-0

[5]. Behzad Razavi (2015). Microelectronics, *John Wiley and Sons, 2015*, ISBN 978-1-118-16506-5

[6]. Bevilaqua, A., and Niknejad, A. m. (2004). An Ultrawideband CMOS Low-Noise Amplifier for 3.1-10.5GHz wireless recveivers. *IEEE Journal of Solid-State Circuits*, *39*(12): 2259–2268.

[7]. Borremans, J., Wambacq, P., Soens, C., Rolain, Y., and Kuijk, M. (2008). Low-Area Active-Feedback Low-Noise Amplifier Design in Scaled Digital CMOS. *IEEE Journal of Solid-State Circuits* 43(11): 2422–2433.

[8]. Brandolini, M., Rossi, P., Manstretta, D., and Svelto, F. (2005). Toward Multistandard Mobile Terminals — *Fully Integrated Receivers Requirements and Architectures*. *IEEE Trans Microw Theory Tech*, *53*(3): 1026–1038.

[9]. Bruccoleri, F., Klumperink, E. A. M., and Nauta, B. (2004). Wide-Band CMOS Low-Noise Amplifier Exploiting Thermal Noise Canceling. *IEEE J Solid-State Circuits*, *39*(2): 275–282.

[10]. Cheng, G., Li, Z., Luo, L., Wang, Z., He, X., and He, B. (2018). A low power and high gain current-reused LNA using cascaded L-type input matching network. *Microelectronics Journal*, 75(2): 15–26. https://doi.org/10.1016/j.mejo.2018.01.021

[11]. Chung, T., Lee, H., Jeong, D., and Kim, B. (2015). A Wideband CMOS Noise-Canceling Low-Noise Amplifier with High Linearity. *IEEE Microwave and Wireless Components Letters* 18(4): 4–6.

[12]. Ebrahimi, A., Bastan, Y., Ebrahimi, E., and Shamsi, H. (2015). Exploiting Cross-Coupled and Body-Driven Techniques for an Noise Cancellation of an Inductorless Widenand LNA. *AEUE - International Journal of Electronics and Communications*. https://doi.org/10.1016/j.aeue.2014.12.014

[13]. Guo, B., and Chen, J. (2017). A wideband common-gate CMOS LNA employing complementary MGTR technique. *IEEE Journal of Solid-State Circuits* 20(3): 1668–1671. https://doi.org/10.1002/mop.30601

[14]. Guo, B., Chen, J., Li, L., Jin, H., and Yang, G. (2017). A Wideband Noise-Canceling CMOS LNA With Enhanced Linearity by Using Complementary nMOS and pMOS Configurations. *IEEE Journal of Solid-State Circuits 1*(c): 1–14.

[15]. Guo, B., Wen, G., and An, S. (2015). 6.8mW 15dBm CMOS Common-gate LNA employing post-linearisation technique. *Electronics Letters* 50(3): 3–4. https://doi.org/10.1049/el.2013.3442

[16]. Hayati, M., Cheraghaliei, S., and Zarghami, S. (2017). Design of UWB low noise ampli fi er using noise-canceling and current-reused techniques. *Integration, the VLSI Journal*, 39(10): 1–8. https://doi.org/10.1016/j.vlsi.2017.10.002

[17]. Huang, D., Yang, X., Chen, H., Khan, M. I., and Lin, F. (2018). A 0.3–3.5 GHz active-feedback low-noise amplifier with linearization design for wideband receivers. *AEU - International Journal of Electronics and Communications*. https://doi.org/10.1016/j.aeue.2017.12.003

[18]. Im, D. (2013). A + 9-dBm Output P 1dB Active Feedback CMOS Wideband LNA for SAW-Less Receivers. *Transactions on Circuits and Systems II : Express Briefs* 2(4): 1–5.

[19]. Jafarnejad, R., Jannesari, A., Nabavi, A., and Saha, A. (2016). A low power low noise amplifier employing negative feedback and current reuse techniques. *Microelectronics Journal* 49(1): 49–56. https://doi.org/10.1016/j.mejo.2015.12.011

[20]. Jafarnejad, R., Jannesari, A., and Sobhi, J. (2017). A linear Ultra Wide Band Low Noise Amplifier using Pre-distortion Technique. *AEUE - International Journal of Electronics and Communications*. https://doi.org/10.1016/j.aeue.2017.05.046

[21]. Lin, Y., S., Chang, J., and Lu, S. (2011). Analysis and Design of CMOS Distributed Amplifier Using Inductively Peaking Cascaded Gain Cell for UWB Systems. *IEEE Transactions on Microwave Theory and Techniques*, 59(10): 2513–2524.

[22]. Ma, L., Wang, Z., Xu, J., and Amin, N. M. (2016). A High Linearity Wideband Common-gate LNA with Differential Active Inductor. *Transactions on Circuits and Systems II : Express Briefs* 7747(c). https://doi.org/10.1109/TCSII.2016.2572201

[23]. Mitola, J. (1995). The Radio Software Architecture. *IEEE Communications Magazine*, 8(5): 26–38.

[24]. Roovers, R., Leenaerts, W., Domine. M., Bergervoet, J., Harish, K. S., Van de Beek, R. C. H., Weide, G. V., Waite, H., Zhang, Y., Aggarwal, S. and Razzell, C. (2005). An Interference-Robust Receiver for Ultra-Wideband Radio in SiGe BiCMOS Technology. *IEEE Journal Of Solid-State Circuits*, 40(12): 2563–2572.

[25]. Sahafi, A., Sobhi, J., and Koozehkanani, Z. D. (2016). Linearity improvement of gm-boosted common gate LNA : Analysis to design. *Microelectronics Journal* 56(8): 156–162. https://doi.org/10.1016/j.mejo.2016.08.015

[26]. Sapone, G., and Palmisano, G. (2011). A 3 – 10-GHz Low-Power CMOS Low-Noise. *IEEE Transactions On Microwave Theory And Techniques*, 59(3): 678–686.

[27]. Seyedi, H., Dehdasht-heydari, R., and Roshani, S. (2019). A novel LNA with noise cancellation in 4–11.5 GHz bandwidth for UWB receivers. *Microelectronics Journal*. https://doi.org/10.1016/j.mejo.2019.04.015

[28]. Vaithianathan, V., Raja, J., and Srinivasan, R. (2012). Low Power, High Gain, Low Noise Amplifier with Improved Noise Figure and Input Matching for Wide Band Applications. *Internal J ournal of Science and Technology*, 36(8): 163-174

[29]. Yusof, N. S., Fauzi, M., Mohamed, P., Faiz, M., and Omar, M. (2020). 28 GHz Off-the-Shelf Low Noise Amplifier for 5G Baseband Wireless System. *International Journal of Innovative Technology and Exploring Engineering (IJITEE)*, *9*(3): 3051–3058. https://doi.org/10.35940/ijitee.C8365.019320

[30]. Zhang, H. S., and Sánchez-sinencio, E. L. (2011). Linearization Techniques for CMOS Low Noise Amplifiers : A Tutorial. *IEEE Transactions on Circuits and Systems.* 58(1): 22–36.